Field Experimental Results on Cooperative Multi-Point Wireless Transmission

Masayuki Miyashita†, Manabu Mikami†, Kenji Hoshino†, Haruya Miyajima†, Hitoshi Yoshino† and Teruya Fujii†
Wireless System R&D Center, Softbank Mobile Corp.
2-5-10 Aomi, Koutou-ku, Tokyo, 135-8070 Japan,
E-mail: †{masayuki01.miyashita, manabu.mikami, kenji01.hoshino,
haruya.miyajima, hitoshi.yoshino, teruya.fujii}@mb.softbank.co.jp

Abstract

For next generation cellular mobile communication systems, cooperative multi-point transmission technologies (CoMP), in which multiple base stations (BSs) coordinate their wireless transmission, have recently been receiving considerable attention due to their potential cell-edge throughput improvement. However, there are few studies that provide field evaluation of cooperative multi-point wireless transmission technologies in real radio-propagation environments. To field evaluate CoMP, BSs located at different sites should be synchronized to each other with high accuracy. We develop a prototype of an experimental system by using a GPS (Global Positioning System)-based inter-BS synchronous controller. We conduct field experiments on two CoMP schemes: (i) cooperative MIMO-SDM based on space division multiplexing and (ii) cooperative MIMO-SFBC based on space frequency block coding. We confirm that CoMP improves the cell-edge throughput performance in real radio-propagation environments. This paper describes the developed field experimental system and the results of the field experiments. It also shows the effectiveness of cooperative multi-point wireless transmission at the cell-edge.

Keywords : Cooperative Multi-Point Transmission, Cell-Edge Throughput, Field Experiment

1. Introduction

In next generation cellular mobile communication systems, such as IMT-Advanced, it is required to improve cell-edge throughput and cell throughput as well as peak throughput [1]. Cooperative multi-point transmission technologies (CoMP), in which multiple base stations (BSs) are synchronized to each other and coordinate their wireless transmission, are receiving considerable attention due to their potential in improving cell-edge throughput [2]. In cooperative multi-point wireless transmission, the radio propagation channels between the transmit antennas at coordinated base stations and the receive antennas at a cell-edge mobile station are regarded as a virtual MIMO (Multiple Input Multiple Output) channel. This channel offers improved channel capacity at the cell-edge.

Most of previous work on CoMP evaluates the wireless transmission performances by computer simulations. Few studies have attempted field evaluations in actual radio-propagation environments. In order to conduct field evaluations, we have developed a prototype of an experimental system for field evaluations, and confirmed its basic radio transmission performance in laboratory experiments with a fading simulator [3], [4]. In implementing CoMP, high-accuracy inter-BS synchronization is an essential requirement. Our field experimental system synchronizes multiple base stations located at different sites each other with high accuracy by using a GPS based inter-BS synchronous controller. We conduct field experiments on two CoMP schemes: (i) cooperative MIMO-SDM based on space division multiplexing and (ii) cooperative MIMO-SFBC based on transmit diversity with space frequency block coding. This paper describes the developed field experimental system and the results of the field experiments.

2. Field Experimental System

2.1 System configuration

Figure 1 illustrates the network configuration of our field experimental system. Table 1 summarizes the key specifications on wireless transmission. The system is composed of two experimental base stations (BSs), each equipped with a transmit antenna, and an experimental mobile station (MS) equipped with two receive antennas. Note that BS #1 and BS #2 are located at different sites. With regard to the antenna configuration, the radio propagation channel between the BS transmit antennas and the MS receive antennas can be regarded as a virtual 2x2 MIMO channel. In the field experimental system, the non co-sited BSs, BS #1 and BS #2, transmit orthogonal frequency division multiplexing (OFDM) signals with the center frequency of 3.3 GHz band, the sub-carrier spacing of 15 kHz, the sub-frame duration of 1 ms and the frame duration of 10 ms. In the field experimental system, the two CoMP schemes, cooperative MIMO-SDM and cooperative MIMO-SFBC, were implemented. The coordinated BSs are synchronized to each other with high accuracy by using a GPS based inter-BS synchronous controller that prevents the timing offset between the received signals of BS #1 and BS #2 from exceeding the Guard Interval (GI) duration of OFDM symbols [3]. The synchronization control can establish inter-BS synchronization even though the base stations are connected to each other via an asynchronous IP (Internet Protocol) network. At each BS transmitter, user data sequences are channel-coded by a turbo-code with coding rate of 1/3. At the MS receiver, the received signals are channel-decoded by the Max Log-MAP algorithm with eight iterations.

Figures 2 (a) and (b) provide block diagrams of the BS transmitter and MS receiver, respectively. Figure 3 illustrates the resource assignment of reference signals for channel estimation at the MS receiver. As shown in Fig. 2 (a), in each BS transmitter, OFDM symbols are generated after each user data sequence is multiplexed with a synchronization signal for timing detection and reference signals for channel estimation at the MS receiver. As shown in Fig. 2 (b), in the MS

receiver, the optimal position of the Fast Fourier Transform (FFT) window is detected from the received signal. The virtual 2x2 MIMO channel is estimated from the received reference signals. Note that the reference signals are orthogonal to the data signals in both the time-domain and the frequency-domain so as to enable high-accuracy channel estimation as shown in Fig. 3. By using the channel estimation result, the desired signal sequences are detected based on the received signal processing described in Subsection 2.2.

2.2 Received Signal Processing at MS receiver

Let $\mathbf{h}_j(k)$ be the frequency channel response for the k-th subcarrier between the j-th BS antenna ($j=1,2$ corresponds to BS #1 and BS #2, respectively) and the MS antennas, the received signal vector at MS, $\mathbf{x}(k)$, can be expressed as

$$\mathbf{x}(k)=\mathbf{H}(k)\mathbf{s}(k)+\mathbf{n}(k), \quad (1)$$

$$\mathbf{H}(k)=[\mathbf{h}_1(k)\ \ \mathbf{h}_2(k)], \quad (2)$$

$$\mathbf{s}(k)=[s_1(k)\ \ s_2(k)]^T, s_j(k)\in\{s_{\text{rep}}^{(m)}\}\ (m=1,\cdots,M_{ary}), \quad (3)$$

$$E\{|s_j(k)|^2\}=1, \quad (4)$$

where $s_j(k)$, $\mathbf{n}(k)$, M_{ary}, $s_{\text{rep}}^{(m)}$, and $E\{\cdot\}$ denote $s_j(k)$ the transmitted signal of j-th BS, the receiver noise vector, the modulation order, the m-th candidate of the transmitted complex symbol value, and ensemble average, respectively.

When cooperative MIMO-SDM is employed, the desired signal sequences are spatially demultiplexed based on minimum mean square error (MMSE) filtering with the channel estimation result at the MS receiver. The output signal of the MMSE filter of the j-th sub-stream, $y_j(k)$, can be expressed as

$$y_j(k)=\mathbf{w}_j^H(k)\mathbf{x}(k), \quad (5)$$

$$\mathbf{w}_j(k)=\{\mathbf{H}^H(k)\mathbf{H}(k)+P_N\mathbf{I}\}^{-1}\mathbf{h}_j(k), \quad (6)$$

where $\mathbf{w}_j(k)$, $\{\cdot\}^H$, P_N, and $\mathbf{I}$ represent the MMSE filter coefficient vector, the conjugate transpose, the average noise density of each receive antenna, and the unit matrix, respectively. The output SINR of the MMSE filter of the j-th sub-stream, $\text{SINR}_{\text{out},j}(k)$, is calculated by [6]

$$\text{SINR}_{\text{out},j}(k)=\mathbf{w}_j^H(k)\mathbf{h}_j(k)\big/\{1-\mathbf{w}_j^H(k)\mathbf{h}_j(k)\} \quad (7)$$

Note that soft-decision channel decoders such as turbo decoders require soft-reliability information such as channel LLR (Log-Likelihood Ratio) of each transmitted bit. Let $c_j(k,l)\in\{0,1\}$ denote the l-th logical bit values of $s_m(k)$. The channel LLR value of each transmitted bit, $L_{ch}(c_j(k,l))$, is calculated as follows [6]

$$L_{ch}(c_j(k,l))=\text{SINR}_{\text{out},j}(k)\left\{\min_{m\in\{s_{\text{rep}}^{(m)}|c_{\text{rep}}^{(m)}(l)=1\}}|y_j(k)-s_{\text{rep}}^{(m)}|^2-\min_{m\in\{s_{\text{rep}}^{(m)}|c_{\text{rep}}^{(m)}(l)=0\}}|y_j(k)-s_{\text{rep}}^{(m)}|^2\right\} \quad (8)$$

where $c_{\text{rep}}^{(m)}(l)\in\{0,1\}$ denote the l-th logical bit of $s_{\text{rep}}^{(m)}$.

When cooperative MIMO-SFBC is employed, the same data sequence is transmitted from both BS #1 and BS #2, The transmitted signal sequence $s(k)$ $(k=2i,2i+1)$ is pre-coded by Alamoti's code and the transmitted signal vector, $\mathbf{s}(k)$ $(k=2i,2i+1)$, can be expressed as [7]

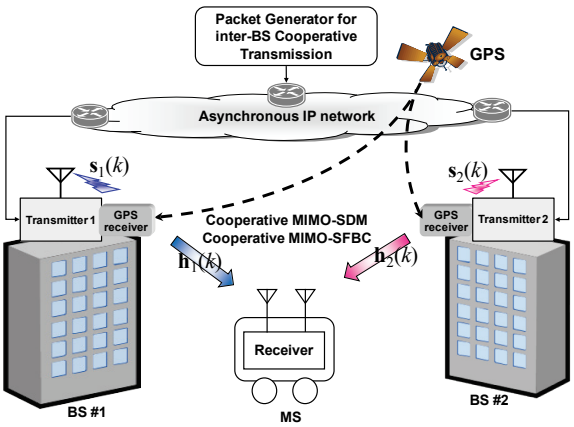

Figure1: Network configuration of the field experimental system.

Table 1: Key specifications on wireless transmission.

Number of BSs/MSs	2/1
Number of antennas	1 (per BS) / 2 (MS)
RF center frequency	3.3GHz band
OFDM parameters	Number of assigned data sub-carriers: 72 Sub-carrier spacing: 15kHz, Guard Interval (GI) duration: 16.67μs,
Sub-frame duration	1ms (12 OFDM symbols)
Frame duration	10ms
Synchronization signal	CAZAC (Zadoff-Chu sequence, PSK)
Reference signal	PN code (Truncated Gold sequence, QPSK)
Data modulation	QPSK, 16QAM, 64QAM
Channel coding	Turbo coding (Constraint lengths = 4, Internal interleaver: Prime interleaver), Coding rate R = 1/3
Multi-point transmission scheme	Cooperative MIMO-SDM Cooperative MIMO-SFBC
FFT timing detection	Peak search of sliding correlation between synchronization signal and received signal
Channel estimation	Time-domain channel estimation with sinc function based channel replica [5]
Signal detection	Cooperative MIMO-SDM: MMSE Cooperative MIMO-SFBC: MRC
Channel decoding	Max Log-MAP decoding (8 iterations)
Block error detection	24 bit cyclic redundancy check (CRC)

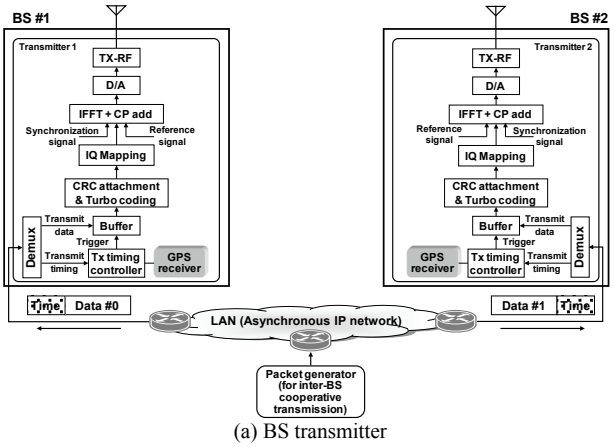

(a) BS transmitter

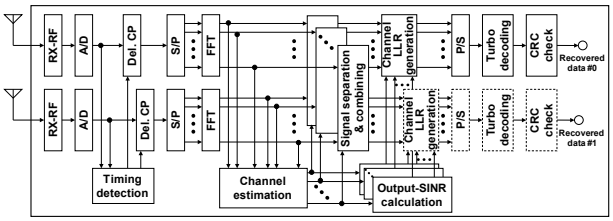

(b) MS receiver

Figure 2: Block diagram of wireless transmission equipment.

$$\mathbf{s}(2i)=\begin{bmatrix} s(2i) \\ s(2i+1) \end{bmatrix}, \mathbf{s}(2i+1)=\begin{bmatrix} -s^*(2i+1) \\ s^*(2i) \end{bmatrix}, \qquad (9)$$

where $\{\cdot\}^*$ denotes the conjugate. From eqs (1), (2), and (9), the following equation is obtained

$$\begin{bmatrix} \mathbf{x}(2i) \\ \mathbf{x}^*(2i+1) \end{bmatrix}=\begin{bmatrix} \mathbf{H}(2i) \\ \mathbf{H}^*(2i+1)\mathbf{P} \end{bmatrix}\begin{bmatrix} s(2i) \\ s(2i+1) \end{bmatrix}+\begin{bmatrix} \mathbf{n}(2i) \\ \mathbf{n}^*(2i+1) \end{bmatrix}, \mathbf{P}=\begin{bmatrix} 0 & -1 \\ 1 & 0 \end{bmatrix}. \quad (10)$$

At the MS receiver, the desired signal sequences are detected based on MRC (Maximum Ratio Combining) with the channel estimation result. Since it is assumed that the difference between adjacent sub-carriers is small enough to be ignored (i.e., $\mathbf{H}(2i+1) \simeq \mathbf{H}(2i)$), the output signal of the MRC signal combiner, $y(k)$ $(k=2i, 2i+1)$, can be expressed as

$$\begin{bmatrix} y(2i) \\ y(2i+1) \end{bmatrix}=\{\mathbf{H}^H(2i)\mathbf{x}(2i)+(\mathbf{H}^*(2i)\mathbf{P})^H\mathbf{x}^*(2i+1)\}\Big/\sum_{j=1}^{2}\left\|\mathbf{h}_j(2i)\right\|^2, \quad (11)$$

The output SINR of the MRC signal combiner, $\mathrm{SINR}_{\mathrm{out}}(k)$, is approximated as

$$\mathrm{SINR}_{\mathrm{out}}(k) \simeq \frac{1}{P_N}\sum_{j=1}^{2}\left\|\mathbf{h}_j(k)\right\|^2. \qquad (12)$$

As in the case of cooperative MIMO-SDM, the turbo decoder requires soft-reliability information such as channel LLR (Log-Likelihood Ratio) of each transmitted bit. Let $c(k,l) \in \{0,1\}$ denote the l-th logical bit values of $s(k)$. Consequently, the channel LLR value of each transmitted bit, $L_{ch}(c(k,l))$, is calculated as

$$L_{ch}(c(k,l))=\mathrm{SINR}_{\mathrm{out}}(k)\left\{\min_{m\in\{s_{\mathrm{rep}}^{(m)}|c_{\mathrm{rep}}^{(m)}(l)=1\}}|\,y(k)-s_{\mathrm{rep}}^{(m)}\,|^2\right.$$

$$\left.-\min_{m\in\{s_{\mathrm{rep}}^{(m)}|c_{\mathrm{rep}}^{(m)}(l)=0\}}|\,y(k)-s_{\mathrm{rep}}^{(m)}\,|^2\right\} \qquad (13)$$

3. Field Experimental Results

3.1 Experimental environment

Figure 4 illustrates the experimental site. The area lies in a typical suburban area in Chofu-city, Tokyo, Japan. In this experiment, BS #1 and BS #2 were placed on buildings separated by about 300m. The BS antennas were mounted on the tops of the buildings with the height of about 30 m from the ground. The MS antennas were mounted on the roof of a van at a height of about 3 m. We first evaluated the BLER (Block Error Rate) performance in a quasi-static environment, i.e., MS was located at the fixed point of "e" in Fig. 4. The radio propagation condition was non-line-of site (NLOS) from both base stations. In the experiment, we also evaluated the throughput performance on the measurement course shown in Fig. 3.

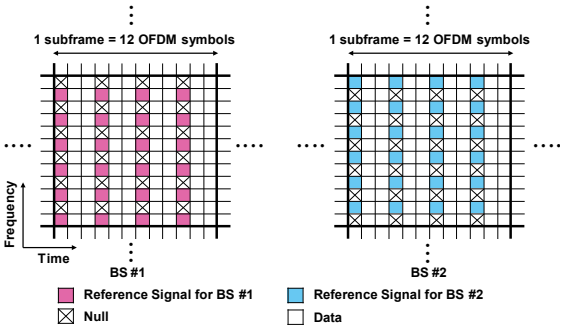

Figure 3: Resource element mapping to reference signals.

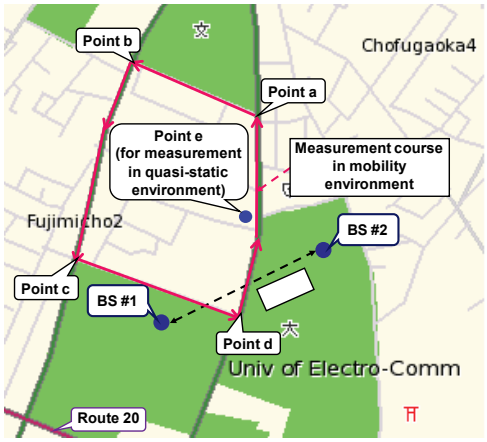

Figure 4: Experimental site.

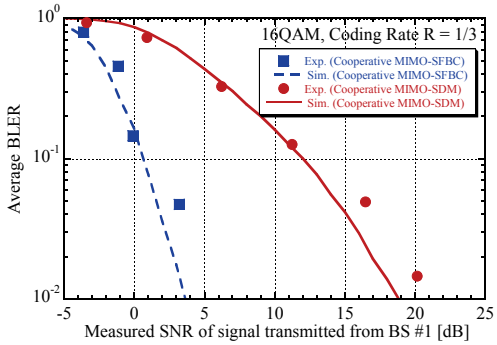

Figure 5: Block error rate performance.

3.2 Experimental results in a quasi-static environment

Figure 5 shows the field experimental results of block error rate (BLER) at point "e", where signals transmitted from BS #1 and BS #2 were received with almost equal power. In this experiment, the transmitted signal was modulated by 16QAM with coding rate of R = 1/3. Instantaneous fading was simulated by moving the van within the short distance of about 3m (corresponds to about 30 wavelengths at the center frequency of the 3.3GHz band). The maximum Doppler frequency was approximately 5 Hz. Delay spread and spatial fading correlation were measured at point "e". The measured delay spread was approximately 0.15 μs. The measured fading correlations between each transmit antenna and each receive antenna were almost 0 (uncorrelated). Figure 5 also shows computer simulation results in which perfect inter-BS synchronization and perfect channel estimation were assumed. In the simulations, the discrete delay path model was generated based on Report ITU-R M.2135 [8] so that the delay spread of the model equals that of the measurement results, and quasi-static fading uncorrelated between each transmit antenna and each receive antenna was generated.

From Fig.5, it is found that the BLER degradation of the field experimental results from the simulation results is less than 2 dB in terms of SNR. The results demonstrate that the field experimental system achieved the intended BLER performance and the implementation of both cooperative MIMO-SDM and cooperative MIMO-SFBC in actual radio-propagation environments.

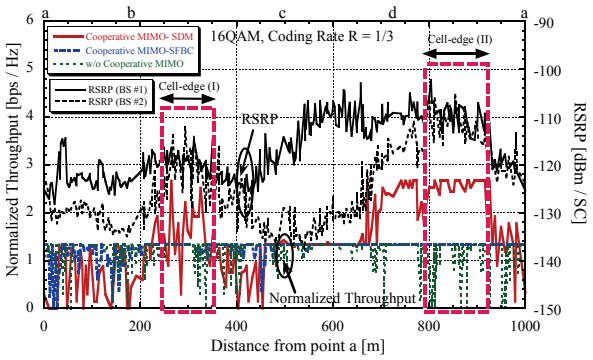

Figure 6: Normalized throughput and RSRP vs. running distance.

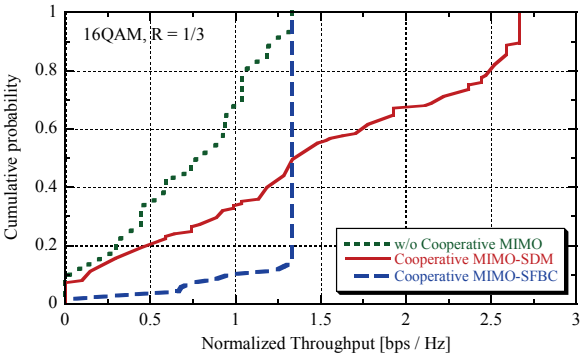

Figure 7: Cumulative probability of cell-edge throughput.

3.3 Experimental results in a mobility environment

Figure 6 plots examples of normalized throughput and RSRP (Reference Signal Received Power per sub-carrier) versus running distance along the measurement course. Since the transmitted signals were modulated by 16QAM (= 4 bits/s) with coding rate of R = 1/3 in the experiment, theoretical maximum throughputs are about 2.6 bps/Hz and 1.3 bps/Hz with and without cooperative MIMO-SDM, respectively. The points of "a", "b", "c" and "d" correspond to the corners of the measurement course shown in Fig. 4. The speed of the van was about 30 km/h. In this experiment, "cell-edge" is defined as the points where the received signal power of BS #1 is approximately equal to that of BS #2. As shown in Fig. 6, "Cell-edge (I)" lies between the 250 m point and the 370 m point. "Cell-edge (II)" lies between the 780 m point and the 930 m point. From Fig. 6, we can conclude that both cooperative MIMO-SDM and cooperative MIMO-SFBC can improve throughputs at the cell-edge relative to the case of without cooperative MIMO. From Fig.6, it is also found that the received signal power at cell-edge (II) is about 10 dB larger than that of cell-edge (I), and that a high signal-to-noise-power-ratio (SNR) is obtained at cell-edge (II). Therefore, at cell-edge (II), both cooperative MIMO-SDM and cooperative MIMO-SFBC almost achieve their theoretical maximum throughputs.

Figure 7 plots the cumulative probability of throughput at cell-edges (I) and (II) (data taken from Fig. 6). For comparison, this figure also plots the characteristics of the case without cooperative MIMO in which BS #2 is set as the interfering BS. For example, we evaluate the throughput values at the cumulative probability of 50 % in the case with cooperative MIMO-SDM, with cooperative MIMO-SFBC and without cooperative MIMO. From Fig. 7, it is found that these values are 1.3 bps/Hz, 1.3 bps/Hz and 0.8 bps/Hz, respectively. This result confirms that both cooperative MIMO-SDM and cooperative MIMO-SFBC can improve cell-edge throughput compared to the case of without cooperative MIMO. Next, we evaluated the throughput values at the cumulative probability of 20 %. From Fig. 7, it is found that cooperative MIMO-SDM improves the throughput value by about 0.8 bps/Hz compared to cooperative MIMO-SFBC. At the cumulative probability of 80 %, Fig. 7 shows that cooperative MIMO-SDM improves the throughput value by about 0.8 bps/Hz compared to cooperative MIMO-SFBC. These results confirm that cooperative MIMO-SDM and cooperative MIMO-SFBC are effective in high and low SNR environments, respectively.

4. Conclusions

We developed a prototype system for field experimental evaluations of cooperative multi-point wireless transmission technologies and conducted a field experiment on (i) cooperative MIMO-SDM based on space division multiplexing and (ii) cooperative MIMO-SFBC based on space frequency block coding, as cooperative wireless transmission schemes. This paper described the developed field experimental system and showed the field experimental results. We confirmed that cooperative wireless transmission is very effective in improving the throughput at the cell-edge.

References

[1] Report ITU-R M.2134, "Requirements related to technical performance for IMT-Advanced radio interface(s)," Dec. 2008.

[2] H. Zhang and H. Dai, "Cochannel interference mitigation and cooperative processing in downlink multicell multiuser MIMO networks," EURASIP Journal on Wireless Commun. and Networking, vol.2004, no.2 pp.222–235, Feb. 2004.

[3] H. Miyajima *et al*., "A prototype system for evaluating multi-cell cooperative transmission in asynchronous mobile radio networks," Proc. IEEE VTC2011-Fall, San Francisco, USA, Sept. 2011.

[4] M. Miyashita *et al*., "A prototype of coordinated multi-BS wireless transmission system," Proc. 2010 IEICE Society Conf., B-5-35, p.389, Sept. 2010.

[5] H. Kayama *et al*., "A study on the accurate channel estimation method applying sinc function based channel replica for a broadband OFDM wireless communication system," IEICE Technical Report, RCS2007-70, Aug. 2007.

[6] D. Seethaler, G. Matz, F. Hlawatsch, "An efficient MMSE-based demodulator for MIMO bit-interleaved coded modulation," Proc. IEEE Globecom2004, pp.2455–2459, Dallas, TX, USA, Nov./Dec. 2004.

[7] G. Li *et al*., "Study on MIMO schemes for 3G-LTE downlink," WSEAS Trans. Commun, vol.8, no.8, pp.883–893, Aug. 2009.

[8] Report ITU-R M.2135, "Guidelines for evaluation of radio interface technologies for IMT-Advanced," Nov. 2008.

Acknowledgments

This work was partially sponsored by the Ministry of Internal Affairs and Communications of Japan, under the grant, "R&D on the cooperative control technologies for multiple base stations in an environment consisting of various cell sizes".